Current Applied Science and Technology Vol. 21 No. 3 (July-September 2021)

Review article

Synthesis of Rare Earth Based Pyrochlore Structured ($A_2B_2O_7$) Materials for Thermal Barrier Coatings (TBCs) - A Review

J. Sankar and S. Suresh Kumar*

Department of Mechanical Engineering, Kalasalingam Academy of Research and Education, Krishnankoil, Tamil Nadu, India

Received: 11 Spetmber 2020, Revised: 7 December 2020, Accepted: 5 January 2021

Abstract

High temperature application requires protection coatings to ensure the optimal operating cycles to avoid the uncertainty caused by hot gases, foreign contaminates, ambient conditions and other occurrences. In general, protective coating materials can be ceramics, thermally grown oxides, silicates and some rare earth ores. For high-end applications such as gas turbines used in aviation, gas turbines surface are coated with a Thermal Barrier Coating to isolate the components thermally and protect the surfaces. Over the past four decades, those coatings have been employed with the inclusion of Yttrium Stabilised Zirconia (YSZ). The up growing developments on those areas require the coating, which can withstand temperatures above 1200°C. Due to this concern, the alternative to the YSZ based coatings finding has been accelerated. Rare earth oxides with pyrochlore structure ceramics are key interest to provide the coating properties comparatively more than YSZ-based coatings. In this paper, the preparation methods for pyrochlore structured ceramics are discussed. A solid state reaction method widely used for preparing the pyrochlore structure ceramics, but it requires higher temperature and long duration. Wet chemical methods such as precipitation, combustion and hydrothermal techniques produce the pyrochlores at lower temperature comparatively than that of solid state reaction-based methods. In coprecipitation method, intermediate hydrates are reduced into pyrochlores by calcinating at higher elevated temperature. Due to the heat treatment at higher temperature, agglomeration occurs. In the combustion synthesis, fuel-induced exothermic chemical reaction results in porous-structured powders. Upon heat treatment, it results in the porous pyrochlore- structured materials with the agglomeration of particles. Hydrothermal synthesis shows high energy efficiency, maximum yield, uniform particle size and morphology. It was understood that microwave-assisted hydrothermal synthesis requires shorter reaction time.

Keywords: thermal barrier coating; solid state reaction; hydrothermal synthesis
DOI 10.14456/cast.2021.47

*Corresponding author: Tel.: (+91) 9894665963
E-mail: sureshme48@gmail.com

1. Introduction

Thermal barrier coatings (TBCs) are generally used to safeguard the components of gas turbine power plants, gas turbine engines, and other hot sections where hot combustion gases with direct interaction [1-3]. Thermal protection coatings are employed to improve the life cycle of those components. Thermal barrier coating material needs to have a high melting temperature, good chemical stabilities from low temperature to high operating temperature, and it should not undergo phase transformation, and sintering during cyclic operation at higher temperature. Moreover, the material should have a low thermal conductivity at higher operating temperature, be well-adherable to substrates, and have a thermal expansion coefficient that matches with the bond coating [4]. Thermal barrier coating generally is employed with a nickel or cobalt-based metallic bond coat that improves the adhesion strength between the substrate and topcoat material. The coating materials are generally rare earth oxides, glasses, rare earth ores, and pyrochlores. A few of those coating materials that are widely used are as follows, zirconia (ZrO_2), alumina (Al_2O_3), lime (CaO), garnet ($Y_3Al_5O_{12}$), mullite, ceria (CeO_2), titanium oxide (TiO_2), lanthanum phosphate ($LaPO_4$), lanthanum aluminate ($LaMgA_{11}O_{19}$), barium zirconate ($BaZrO_3$), lanthanum zirconate ($La_2Zr_2O_7$) (LZ) and yttria stabilised zirconia (YSZ) [5]. Figures 1 and 2 show the melting temperature, the thermal expansion coefficient of the various above-discussed coating materials.

ZrO_2, CeO_2, and YSZ having high thermal expansion coefficient, which nearly match that of the NiCoAlY based Band Coat (BC) ($\alpha_{BC} = 17.5\times10^{-6}K^{-1}$) [6-8]. ZrO_2, YSZ, and Ba_2ZrO_3 having a higher melting temperature. YSZ, mullite, YSZ + CeO_2 coatings have excellent thermal shock resistance [9]. Silicates, alumina and mullite show higher corrosion resistance at higher working temperatures [10]. ZrO_2, YSZ, mullite, and alumina undergo phase transformation at higher temperature [11]. Mullite, alumina, $La_2Zr_2O_7$, and silicates have a very low thermal expansion coefficient [12]. ZrO_2, YSZ, and CeO_2 coating sinter at a higher temperature. ZrO_2 coating at higher temperatures shows a high level of oxygen transport to the BC, which causes thermally grown oxide (TGO) layer formation on the surfaces, leads to the spallation of ceramic coating and thus coating failure. YSZ has been commonly used as TBC material for the past four decades [13].

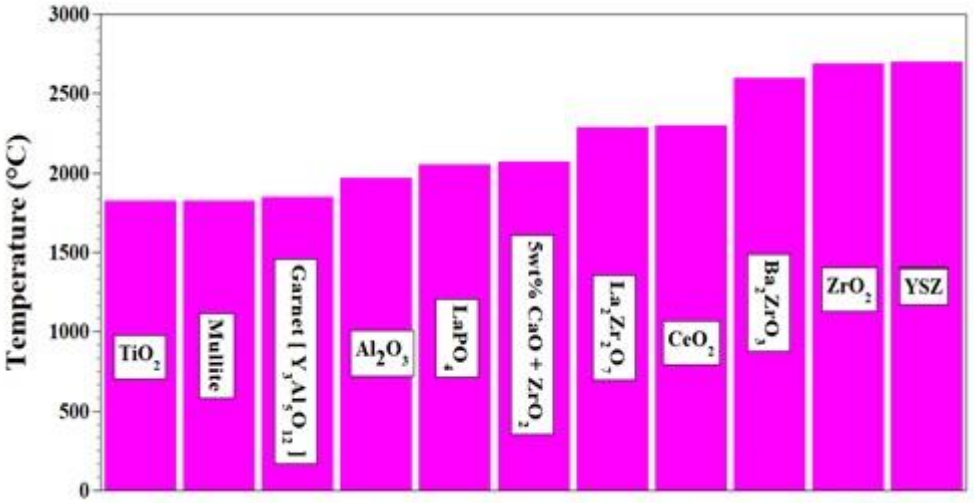

Figure 1. Melting temperature of various coating materials

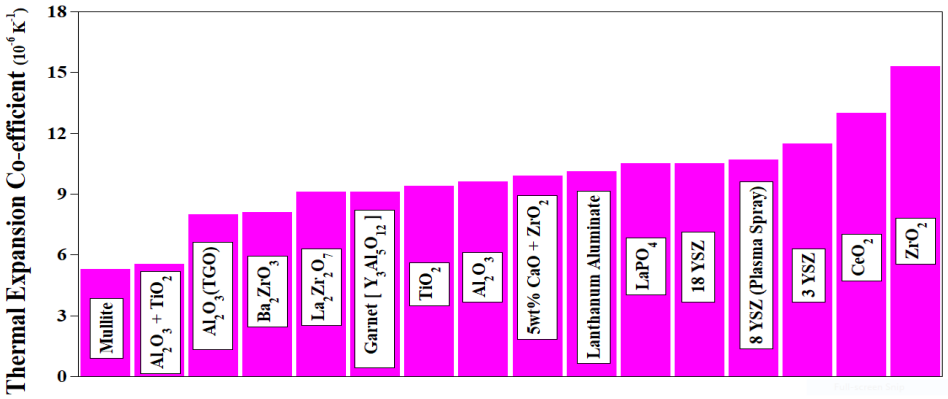

Figure 2. The thermal expansion coefficient of coating materials

At temperature beyond 1200°C, YSZ changes its crystal structure from tetragonal phase to tetragonal + cubic phase and then to monoclinic crystal structure [14]. As a consequence, at temperature above 1200°C, the volume of the coating material phase changes increases and sintering occurs due to this the reduction in thermal conductivity, which in turn leads to strain on the coating that results in cracking and prone to failure of coatings [15]. Undesirable phase transformation occurs at higher temperatures due to incomplete combustion of gases and air pollution [16].

For components operating under humid environment, and at low temperature, slow and spontaneous phase transformation from tetragonal to monoclinic at low temperature can occur. The above occurring phenomenon is known as low-temperature ageing degradation (LTAD) [17]. In the case of CeO_2 doped YSZ coating, the thermal stress generated at higher temperature closely matches the stress that develops on BC and shows higher and excellent thermal shock resistance, and the thermal expansion coefficient also increases more than YSZ [18]. Moreover, the CeO_2 doped YSZ coating reduces the hardness of the coating, and the vaporization of CeO_2 at higher operating temperatures leads to an accelerated sintering rate [19].

Pyrochlore structures are used in a vast range of applications such as catalysis, nuclear waste management, hydrogen production, sensors, and thermal barrier coatings. This is due to their unique crystal structure, thermal stability from room temperature to higher operating temperature, lower thermal conductivity at a higher temperature and good ionic conductivity. The pyrochlore structure belongs to the Fd-3m space group where A sites are occupied by mono, di and tri-valent rare earth cations and B sites are occupied by 3d, 4d and 5d transition metal cations. Among all the above oxidization states, $A^{3+}{}_2B^{4+}{}_2O_7$ species are widely preferred due to their stable ionic radius ratio [20].

Table 1 shows the various rare earth elements cationic radiuses in Å. Many of the rare earth elements have different RE^{3+} and RE^{4+} oxidization states, and those cationic radiuses are also mentioned in Table 1.

Lanthanum zirconates (LZ) contains two crystal structures that can be classified as ordered pyrochlore and disorder fluorite [21]. The type of crystal structure is based on the annealing temperature and the ratio of the crystal structure ionic radius of $r(Re^{3+})/r(Zr^{4+})$ [22]. In pyrochlore structures, the ratio lies between 1.46 and 1.78 [23]. LZ with the pyrochlore structure shows a longer thermal cycling life. The pyrochlore-structured materials have $A^{3+}{}_2B^{4+}{}_2O_7$ structure. Rare earth lanthanum, gadolinium, samarium, and neodymium can be substituted into "A" lattice site, and zirconium, cerium, and titanium may be situated on "B" sites. In recent days, researchers have also investigated co-doped pyrochlore for TBCs.

Table 1. Ionic radius of A^{3+} and B^{4+} cations

A cation	r(A^{3+}) in Å	B cation	r(B^{4+}) in Å
Yb	0.985	Ru	0.62
Er	1.004	Nb	0.68
Y	1.019	Ta	0.68
Dy	1.027	Hf	0.71
Gd	1.053	Zr	0.72
Eu	1.066	Ce	0.87
Sm	1.079	Y	0.90
Nd	1.109	Eu	0.947
Ce	1.143	Sm	0.958
La	1.16	Sc	0.745
Pr	1.126		

In this review work, the various possible synthesis routes available to prepare the rare earth-based pyrochlore structured materials for thermal barrier coatings are explored. The most widespread solid-state reaction is discussed initially with recently reported research work. In addition to this, the bottom-up wet chemical synthesis routes, namely coprecipitation, hydrothermal, sol-gel and combustion methods are discussed. Moreover, the thermomechanical properties of the synthesis materials are also explored in the article.

2. Preparation of Pyrochlore

The preparation of the pyrochlore structured TBC materials can be done by following methods: solid-state reaction, sol-gel method, solution reaction method, co-precipitation method, hydrothermal synthesis method and hydrazine methods [24]. The solid-state reaction method is widely used to synthesize pyrochlore in larger quantity, and the preparation of pyrochlore requires temperature above 900°C. Pyrochlore synthesized by the solid-state reaction displays heterogeneous mean particle size, and it gets easily agglomerated during heat treatment and sinters at very high temperatures. Wet chemical synthesis, on the other hand, involves synthesis of pyrochlore at the molecular level, so it provides powers with uniform particle size. Hydrothermal synthesis enables the preparation of pyrochlore at lower temperature than the solid-state reaction. Researchers also found the use of surfactants in hydrothermal synthesis that reduces the reaction temperature, pH, reaction time duration. Sol-gel methods, co-precipitate method, and hydrazine methods are also used to prepare the hydrates of the corresponding pyrochlore. Sintering process at higher temperatures results in the production of the required pyrochlore materials.

2.1 The solid state reaction method

In the solid-state reaction method (Figure 3), the rare earth oxide mixture at required stoichiometry is preheated to remove moisture and other impurities for about 120°C for 2 h. The resultant mixture is ball-milled for 15 min to form a uniform mixture immersion with distilled water or absolute ethanol. The resultant colloidal mixture heat treatment/calcination/sintering is carried out at above 1500°C to obtain the required pyrochlore structure. Researchers [25-27] also reported the ball milling and sintering process needed to be repeated a few times to obtain the required uniform pyrochlore structure.

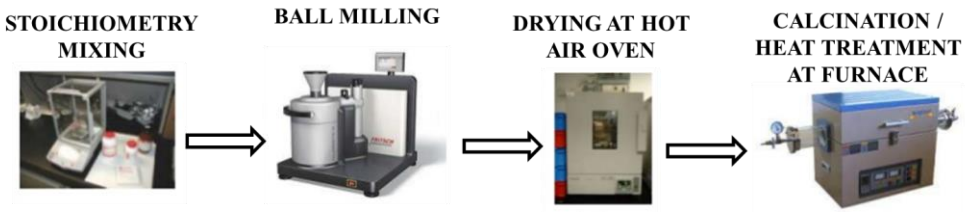

Figure 3. Pictorial representation of solid-state reaction method

Zhong *et al*. [27] prepared gadolinium zirconate (GL) pyrochlore powders through the solid-state reaction by sintering powder at 1500°C for 12h. Zhou *et al*. [28] prepared GZ pyrochlore for TBC using their respective oxides Gd_2O_3 and ZrO_2 stoichiometry and milled mixture dissolving in absolute ethanol, with a small amount of polyethyleneimine added after milling and the resultant mixture suspension diluted with 5 wt% of ethanol before coating. Lehmann *et al*. [29] prepared lanthanum rare earth element zirconate pyrochlore using a solid-state reaction method. Stoichiometric quantities of lanthanum oxides and ZrO_2 preheated at 1200°C for 2 h were taken at required composition and added to ethanol for ball milling for 24 h in a planetary milling using zirconia containers and balls. The resultant powder, after drying underwent a solid-state reaction at 1400°C for 24 h in zirconia crucible.

Ma *et al*. [25] prepared rare earth-codoped strontium zirconate pyrochlore by using a solid-state reaction. The rare earth oxides Y_2O_3, Yb_2O_3, $SrCO_2$, and ZrO_2 powders were mixed by milling for 24 h with 50 wt% water using zirconia balls. The milled powder water mixture was dried at 1450°C for 24 h and milled 15 min to avoid contaminations. The synthesis procedure was repeated until the required phase material had formed. Zhong *et al.* [30] prepared gadolinium zirconate by a solid-state reaction. Gd_2O_3 and ZrO_2 underwent a solid-state reaction at about 1500°C for 12 h. Ma *et al.* [31] prepared Ta_2O_5 and Yb_2O_3 codoped strontium zirconate using a solid-state reaction. The ball-milled powders were sintered at 1450°C for 24 h and the process was repeated three times to obtain the required phase material formation. The resultant powders were cold-pressed under a pressure of 30 MPa and the sintering process was carried out at 1700°C for 6 h in ambient air.

Li *et al*. [32] prepared lanthanum zirconate pyrochlore powder using a solid-state reaction. La_2O_3 and ZrO_2 powders were ball-milled for 24 h using zirconia balls with DI water and the resultant suspension was sintered at 1400°C for 12 h. Hu *et al*. [33] prepared Nd and Ce codoped $Gd_2Zr_2O_7$ pyrochlore ceramic using a solid state reaction. All the rare earth oxides were preheated at 120°C for 3 h to remove moisture and impurities, taken at the required ratio, and milled by grinding. The ground powder was compacted into pellet form under 10 MPa pressure and sintered at 1500°C for 72 h to perform the solid-state reaction. Mazilin *et al*. [34] prepared $Ln_2Zr_2O_7$ Zirconates using a solid-state reaction. Zirconium, neodymium, samarium, and gadolinium nitrate solutions were prepared separately and mixed gravimetrically. The mixture solution was fed into a spray reactor heated by hot air. The resultant powder was collected using a bag filter. Pasupuleti *et al*. [35] prepared lanthanum zirconate, lanthanum cerium zirconate, and cerium zirconate pyrochlore powder using a solid-state reaction. Table 2 shows the various rare earth-based pyrochlores' thermal expansion coefficients.

Wang *et al*. [36] prepared ytterbium cerium oxide by zirconate doping using a solid-state reaction involving sintering at 1500°C for 5 h. Yang *et al*. [38] prepared rare earth zirconate with cerium doping using a solid state reaction. The powders were preheated at 1000°C for 5 h, and then Yb_2O_3, ZrO_2, and CeO_2 were ball-milled with ethanol at the required composition using planetary ball mill for 12 h at 300 rpm and calcined at 1000°C for 5 h. Ma *et al*. [26] prepared strontium

Table 2. The thermal expansion coefficients of various pyrochlores prepared by solid-state reaction

Material	Coefficient of thermal expansion in ($\times 10^{-6}$ K^{-1})	Reference	Material	Coefficient of thermal expansion in ($\times 10^{-6}$ K^{-1})	Reference
$Gd_2Zr_2O_7$	10.4	[25]	$Yb_2(Ce_{0.5}Zr_{0.5})_2O_7$	11.4	[35]
$La_2Zr_2O_7$	9.1	[27]	YSZ	11	[35]
$La_{1.7}Dy_{0.3}Zr_2O_7$	8.8	[27]	$La_2Ze_2O_7$	9.1	[35]
$La_{1.4}Nd_{0.6}Zr_2O_7$	8.2	[27]	$Sr_2Zr_2O_7$	9.0 to 10.8	[36]
$La_{1.4}Eu_{0.6}Zr_2O_7$	9.3	[27]	$Yb_2Zr_2O_7$	11.1	[37]
$La_{1.4}Gd_{0.6}Zr_2O_7$	9.35	[27]	$Yb_2(Zr_{0.9}Ce_{0.1})_2O_7$	11.5	[37]
$Gd_2Zr_2O_7$ – 3 YSZ	10.6	[29]	$Yb_2(Zr_{0.7}Ce_{0.3})_2O_7$	11.75	[37]
$Yb_2Ce_2O_7$	11.8	[35]	$Yb_2(Zr_{0.5}Ce_{0.5})_2O_7$	12	[37]
$Yb_2(Ce_{0.9}Zr_{0.1})_2O_7$	11.7	[35]			

zirconate codoping with double rare earth oxide using a solid-state reaction. ZrO_2 and Yb_2O_3 underwent heat-treatment at 1000°C for 2 h and $SrCO_3$ was added and ball-milled for 24 h using zirconia balls with DI water. The resultant mixture was heat-treated at 1400°C for 24 h. The above ball milling and heat treatment was repeated until the single-phase pyrochlore structures were formed [38]. Pasupuleti *et al*. [39] prepared LZ, LC, and LZ – C zirconate using a solid-state reaction method.

2.2 Coprecipitation method

The coprecipitate method (Figure 4) is a wet chemical synthesis route and easy method to prepare pyrochlore structure after the solid-state reaction method. In this method, the rare earth nitrate salts were dissolved in DI water and the rare earth oxides were dissolved in acid and then the two solution were mixed. The pH was increased to about 9.0 to 11.0 for the above mixture using ammonia or sodium hydroxide, resulting in the formation of rare-earth complex hydrates. The heat treatment and sintering reduce the hydrates into uniform pyrochlore structures.

Zhang *et al*. [40] prepared amorphous lanthanum zirconate pyrochlore using a wet chemical co-precipitate method. Zirconate oxychloride and lanthanum nitrate salts were taken as starting materials, and ammonia was used as a pH stabilizer to raise pH to more than 9. The resultant solution stirring for 24 h resulted in a gel-like precipitate. The filtered and washed precipitates at pH 7 were initially dried at 80°C for 12 h and heat-treated at 300°C for 1 h. Liu *et al*. [41] prepared ytterbium and samarium oxide codoping zirconate pyrochlore using the co-precipitate method. The rare earth oxides of ytterbium and samarium were preheated at 900°C for 2 h to remove the impurities and dissolved in dilute nitric acid. Zirconia oxychloride was dissolved in DI water and all solution mixed with stirring then filtered. The filtered solution pH was increased by adding diluted ammonia solution with stirring resulting in the formation of gel-like precipitates. The resultant precipitates were rinsed and filtered with water and ethanol a few times. The resultant powder was dried and heat-treated at 800°C for 5 h in the air. The heat-treated powder underwent compacting and sintering at 1700°C for 10 h in the air. Zhou *et al*. [42] prepared rare earth codoping on lanthanum zirconate using the co-precipitate method. Lanthanum oxide was dissolved in hydrous nitric acid and zirconia oxychloride was dissolved in DI water mixed and the mixture was stirred for 30 min. Aqueous ammonia added to the above mixture solution to obtain a pH of 12.5, and

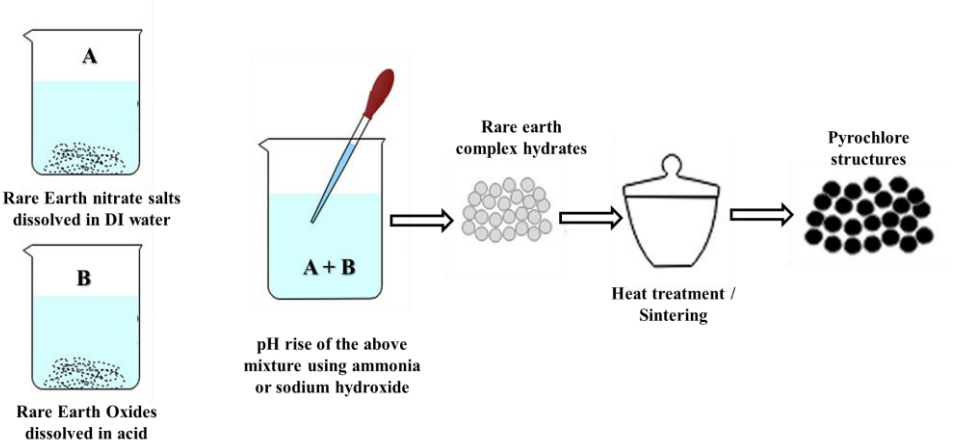

Figure 4. Pictorial representation of coprecipitation method

a gel-like precipitate formed. The precipitates was filtered, washed, and dried at 120°C for 12 h, heat-treated at 600°C for 10 h and calcinated at 1200°C for 5 h.

Gentleman *et al*. [43] prepared europium doped zirconate and YZ using the reverse co-precipitate method. Europium nitrate and yttrium nitrate salt solution, zirconium acetate solution were prepared in DI water. The mixture of all the solution resulted in the formation of a precipitate. The dried precipitates were heat-treated at 950°C and sintered at 1200°C for 2 h. Torres-Rodriguez *et al*. [44]. prepared $Ln_2Zr_2O_7$ (Ln = La, Nd, Dy, and Gd) pyrochlore powders using the co-precipitate method. Ln nitrate salts and zirconium oxychloride were dissolved separately in water with stirring for 30 min and then mixed with further stirring for 2 h. Aqueous ammonia solution used as the pH stabilizer to reach pH of 11 resulted in the formation of precipitates. The precipitates were rinsed with water and dried at 120°C for 12 h. Heat treatment was carried out at 1000°C in the air for 5 h to obtain the $Ln_2Zr_2O_7$ powder.

Bencina *et al*. [45] prepared $Bi_2Ti_2O_7$ pyrochlore using the co-precipitate method. $Bi(NO_3)_3{\cdot}5H_2O$ was dissolved in acetic acid with 20 min stirring and titanium isopropoxide was added to the above solution mixture and stirred for 5 min. Ammonium hydroxide solution was added dropwise to obtain a white-coloured precipitate. The precipitate was rinsed with water and dried at 100°C for 3 h. The dried powder was heat-treated at 550°C for 5-12 h. Gupta *et al*. [46] prepared Eu^{3+} doped $La_2Hf_2O_7$ using the co-precipitate method and MSS procedure with varying pH.

Kaliyaperumal *et al*. [47] prepared $Nd_2Zr_2O_7$ using the co-precipitation method. Neodymium nitrate, zirconium oxychloride were dissolved with Di water, and ammonia solution was added to adjust the pH to 11, which resulted in the formation of a precipitate. The precipitates was washed with water, ethanol and dried at 100°C and heat-treated at 800°C, 1000°C, 1200°C, and 1300°C. Pokhrel *et al*. [48] prepared pyrochlore Rare Earth Hafnate $RE_2Hf_2O_7$ (RE = La, Pr) using the co-precipitate method. Popov *et al*. [49] prepared $Ln_2M_2O_7$ (Ln = Gd, Tb, Dy; M = Ti, Zr) pyrochlore using coprecipitate method. Wang *et al*. [50] prepared rare earth-substituted $Ln_2Sn_2O_7$ pyrochlore (Ln = La, Nd and Sm) using the co-precipitation method. Rare earth nitrate and $SnCl_4{\cdot}5H_2O$ were dissolved in water, and NaOH aqueous solution added to the mixture to reach pH 9.5 ± 0.5 under vigorous stirring for 1hr. The resultant precipitate and mother liquor were aged at 50°C for 2 h and filtered. The filtered powder was washed and dried at 80°C for 12 h and then 120°C for 12 h before heat treatment at 900°C for 6 h in the air atmosphere. Table 3 shows the various rare

Table 3. Thermal conductivity, thermal diffusivity and hardness of pyrochlores prepared by coprecipitation

Material	Thermal conductivity in W/m·K	Thermal diffusivity in mm^2/s	Hardness in GPa	Reference
$Pr_2Zr_2O_7$	0.7	2.75	9.9	[48]
$Sm_2Zr_2O_7$	0.49	2.5	9.8	[48]
$(PrSm)_2Zr_2O_7$	0.38	1.25	8.9	[48]

earth-based pyrochlores' thermomechanical properties and significant pyrochlores suitable for thermal protection coatings.

2.3 Combustion method

The combustion method is similar to the precipitation technique described above; however, the use of fuel source and oxygen source results in auto-ignition and thus the production of pyrochlore powders. The fuel chemical agent was glycine, hydrazine, citric acid, and glycerol. The post-heat treatment of the fluffy powder removes the impurities and results in the required pyrochlore structure powders.

The combustion method (Figure 5) gives high efficiency, involves a simple reaction with low energy consumption, and produces powders with uniform morphology. The combustion method produces pyrochlore powder with a highly porous structure.

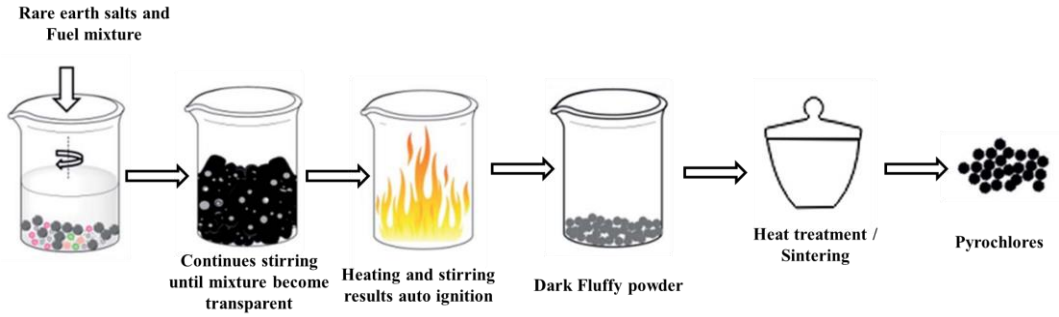

Figure 5. Pictorial representation of combustion method.

Matovic *et al*. [51] prepared lanthanum zirconate, dissolving lanthanum nitrate, zirconium chloride in glycine. The resultant solution was heat-treated at 950°C for 2 h then sintered at 1600°C for 4 h. Venkatesh *et al*. [52] prepared cerium zirconate using the combustion synthesis method. Cerium nitrate and zirconium nitrate solution were prepared by dissolving it in nitric acid and stirring for complete dissolving. Glycine was dissolved separately in DI water before adding dropwise to the cerium-zirconium mixture at a slow stirring rate and stirring was continued for 45 min with mild heat. This resulted in solution becoming transparent. The transparent solution was transferred to an alumina crucible and kept in a muffle furnace at 650°C for 10-15 min. the resultant powder was sintered at 1100°C to form $Ce_2Zr_2O_7$.

Li *et al*. [53] prepared $Gd_2Zr_2O_7$ transparent ceramic using the combustion synthesis method under vacuum sintering. $Gd(NO_3)_3{\cdot}6H_2O$ and $Zr(NO_3)_4{\cdot}5H_2O$ were dissolved in water and hydrous ammonia added to the mixture. The mixture was heated until the gelatine formed, and then

it was transferred to a muffle furnace and heated at 300°C until a fluffy grey powder formed. The powder was calcinated at 1200°C for 2 h and ball-milled for 24 h with DI water. The slurry was dried, pelleted and sintered at 1775°C, 1800°C, and 1825°C for 6 h in a vacuum and annealed at 1500°C for 5 h in the air. Jeyasingh *et al*. [54] prepared $Gd_2Ti_2O_7$ using the combustion process. Gd_2O_3 and TiO_2 were dissolved in nitric acid and mixed with distilled water and citric acid added with stirring for uniform mixing. Nitric acid and ammonium hydroxide were added to the above mixture to adjust the oxygen fuel ratio. The complex mixture at pH 7 was heated at 250°C. Dehydration followed by decomposition resulted in a dark form that auto-ignited, which resulted in voluminous and fluffy combustion powder. The fluffy combustion powder was calcinated at 600°C to remove the carbon residues.

Jeyasingh *et al*. [55] prepared $Dy_2Ti_2O_7$ pyrochlore oxide using combustion synthesis. Dy_2O_3 and TiO_2 were dissolved in nitric acid and mixed with diluted citric acid with stirring at room temperature. Ammonium hydroxide was added to increase the pH to 7 pH 7 and match the oxygen fuel ratio. Heating at 250°C resulted in auto-ignition and a dark fluffy powder. The powder was then calcinated at 700°C, pelleted and sintered at 1400°C for 4 h. $A_2Ti_2O_7$ (A = Gd, Dy and Y) pyrochlore oxide was also prepared using the combustion synthesis method. Ai *et al*. [56] prepared Ca–Co dually-doped lanthanum tin pyrochlore oxide using the combustion synthesis method. $SnCl_4 \cdot 5H_2O$ and $Co(NO_3)_3 \cdot 6H_2O$ were dissolved in DI water and heated at 80°C. Sodium hydroxide was added to the above mixture and this resulted in the white-coloured precipitate. $La(NO_3)_3 \cdot 6H_2O$ and $CaCl_2$ were dissolved in DI water and heated at 80°C. Sodium hydroxide was added to the above mixture and white colour precipitate formed. The above two precipitates were mixed, and pH adjusted to 10 by adding additional sodium hydroxide solution. CTAB was added at 1:1 ratio with metal ions by rapidly dissolving under sonication. The mixture was heated at 80°C for 5 h in an underwater bath and then heated at 80°C for 24 h. The precipitate was filtered and dried at 110°C overnight and calcinated at 900°C for 6 h in the air [57].

Quader *et al*. [58] prepared Nd–substituted $La_2Sn_2O_7$ pyrochlore using sol-gel auto combustion. $La(NO_3)_3 \cdot 6H_2O$, $Nd(NO_3)_3 \cdot 6H_2O$, $SnCl_4$ precursors, and fuel agents NH_2CH_2COOH and CH_4N_2O were dissolved separately in DI water with 2:1 ratio of fuel and precursors. The solution was mixed in a single beaker, heated at 90°C, and stirred at 300 rpm using a magnetic stirrer to obtain a viscous solution. The solution was further heated at 180°C to form paste-like colloid, and again increased up to 260°C which formed exothermic reaction that produced a fluffy powder. The fluffy powder was ground into a fine powder and calcinated at 600°C for 3 h. The calcinated powder was pelleted and sintered at 400°C for 1 h.

Zhang *et al*. [59] prepared a $(Gd_2\text{-}XCe_x)Ti_2O_7$ pyrochlore structure using the combustion method. Tetra butyl titanate, Gd_2O_3, $Ce(NO_3)_3 \cdot 6H_2O$ were used as precursors and glycerol was used as fuel. $Ce(NO_3)_3 \cdot 6H_2O$ was dissolved in water, Gd_2O_3 was dissolved in nitric acid and then heated to remove the excess amount of nitric acid and then all three prepared precursor solutions are combined. Tetra butyl titanate was added dropwise resulting in the formation of a precipitate. The appropriate amount of citric acid was added to the mixture solution and stirred until complete dissolution was achieved. The solution was heated at 200°C with stirring resulted in a gel-like solution and further dehydration resulted in auto-ignition that left behind voluminous powder. The resultant powder was calcinated at 1200°C for 2 h.

2.4 Hydrothermal method

In hydrothermal synthesis (Figure 6), the reaction precursors at required composition are dissolved with a suitable solvent, mixed by stirring and pH of the mixture solution is raised above 7 by using agents like ammonium hydroxide and sodium hydroxides. The clear transparent solution is then

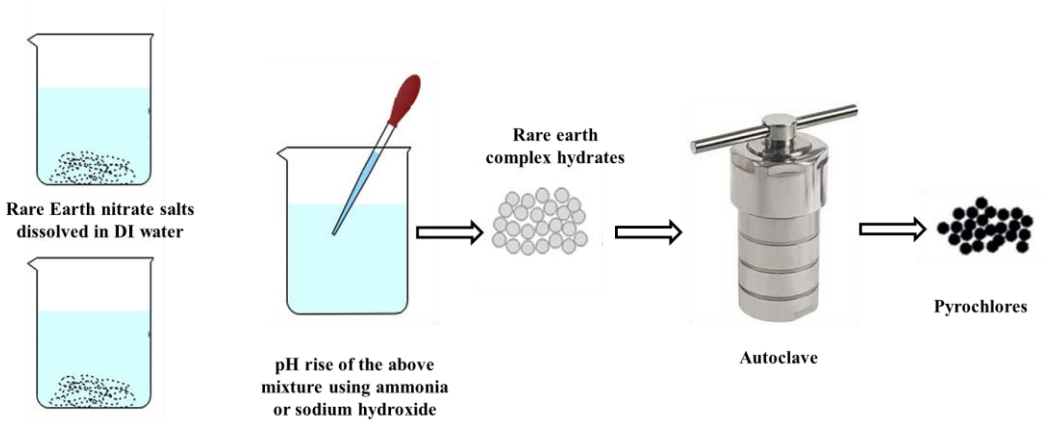

Figure 6. Pictorial representation of the hydrothermal synthesis method

transferred to the hydrothermal reaction chamber for the processing of hydrothermal synthesis. The hydrothermal synthesis method is the only method, which uses a lower reaction temperature (below 400°C) than other methods. The hydrothermal synthesis consumes long reaction duration, the reaction time depends on the pH of the solution. Surfactants are also used to reduce reaction time. Microwave-assisted hydrothermal synthesis features reduced reaction time.

Wang *et al*. [60] prepared $Sm_2Zr_2O_7$ pyrochlore using hydrothermal synthesis. SmO_2 and $ZrOCl_2{\cdot}8H_2O$ were dissolved in HNO_3 and stirred for 10 min. Aqueous ammonia was added to the above mixture to obtain pH 5-9, which resulted in the formation of a white precipitate. The precipitates was washed, and KOH solution was added with vigorous stirring and the mixture was transferred into a teflon-lined autoclave. A hydrothermal reaction was carried out at 100°C and 200°C. The resultant powder was washed and dried at a vacuum at 70°C for 18 h.

Hongming and Danqing [61] prepared lanthanum zirconates using lanthanum and zirconate nitrate salts, and NaOH was used to raise the pH to 11, and a hydrothermal reaction was then carried out at 200°C for 1 h. Huo *et al*. [62] prepared $Ce_2Sn_2O_7$ using hydrothermal synthesis. Cerium nitrate and sodium stannite hydrate were dissolved in DI water, and pH was adjusted by NaOH and stirring for 10 min. The mixture was transferred into a teflon-lined stainless steel autoclave for hydrothermal synthesis. Gadipelly *et al*. [63] prepared $Y_2Ti_2O_7$ pyrochlore structure using microwave-assisted hydrothermal synthesis. Y_2O_3 and TiO_2 were dissolved in preheated nitric acid, and the pH of the mixture increased to 12 by adding NaOH. The mixture underwent microwave-assisted hydrothermal synthesis for 4 min. The resultant precipitates was dried and calcinated at 800°C-1050°C for 3 h.

Sanjeewa *et al*. [64] prepared rare earth pyrochlore germinates $RE_2Ge_2O_7$ (RE = Yb and Lu) using high-temperature hydrothermal synthesis. RE oxides and germinate oxides were loaded into silver ampules and mineralizer solution added and then welded and sealed. The ampules were kept in a hydrothermal chamber and the remaining volume was filled with DI water, sealed, and heated at 600°C for 14 days. Trujillano *et al*. [65] prepared $Sm_2Sn_2O_7$ pyrochlore using accelerated microwave-assisted hydrothermal synthesis. $Sm(NO_3)_3{\cdot}5H_2O$ and $SnCl_4{\cdot}5H_2O$ were dissolved in water and mixed with NaOH solution to increase the pH to 9, resulting in precipitates. The precipitate slurry was mixed for 24 h at room temperature and transferred to a teflon container and hydrothermal synthesis was carried out at 200°C for 4 h. The resultant powder was dried at 40°C for 8 h and 140°C for two days.

2.5 Sol-gel method

The sol-gel method (Figure 7) is one of the wet chemical synthesis methods used to prepare porous-structured materials that are composed of three-dimensional polymeric chains for a wide range of applications. The sol-gel process, which involves hydrolysis followed by condensation, results in synthesis of a gel-like substance with a repentant polymeric matrix, and the drying heat treatment results in the dense powders.

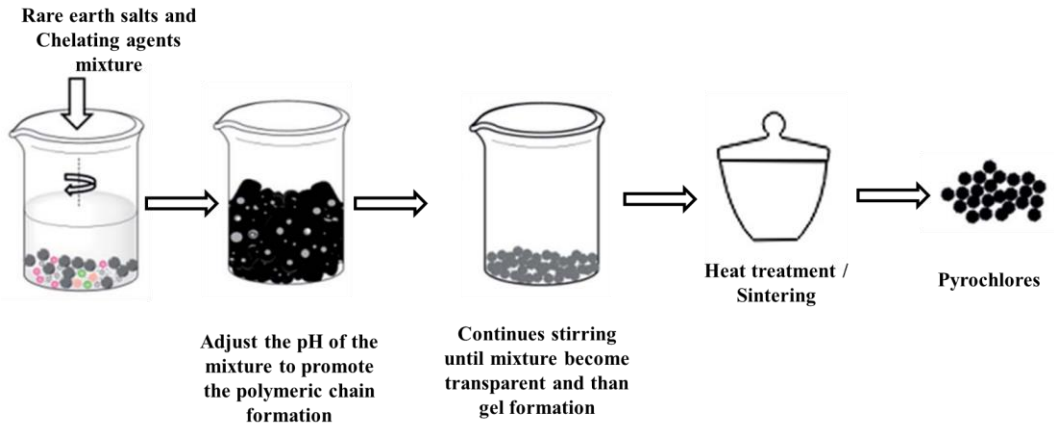

Figure 7. Pictorial representation of sol-gel method

Verma *et al*. [66] prepared rare earth titanate $RE_2Ti_2O_7$ (RE = Dy, Sm) crystal structure pyrochlore using the sol-gel method. $Ti(OiPr)_4$: EtOH : AcAc = 1: 27: 0.5 molar ratio and $RE(NO_3)_3 \cdot XH_2O$: EtHO = 1 : 10 molar ratio sol solutions were prepared separately by stirring for 30 min. The above two sol solutions were added together and stirred for 15 min and HNO_3 was added as a catalyst to promote hydrolysis. Additional DI water added to the above mixture to aid gel formation. The resultant gel was aged for 7 days and dried at 120°C for 48 h to obtain powder that was then annealed at 875°C for 4 h. Wang *et al*. [67] prepared $La_2Zr_2O_7$ pyrochlore using the sol-gel process and slurry. $ZrOCl_2 \cdot 8H_2O$ and $La(NO_3)_3 \cdot 6H_2O$ were dissolved in H_2O/EtOH solution mixed. Citric acid was added to the above mixture to achieve Zr^{4+} : La^{3+} : CA = 1: 1: 0.2. Chelating agent formamide (FA) and polyethylene glycol were added to the above mixture, which was then stirred at room temperature for 2 h to form uniform transparent sol solution. The resultant solution powder was put into a crucible and kept at 80°C for 20 h ageing, which resulted in gel formation. The resultant gel was dried at 110°C for 5 h and calcinated at 1200°C for 2 h in a muffle furnace to form homogeneous $La_2Zr_2O_7$ powders. Xia *et al*. [68] prepared Yb/Er/Eu: $Gd_2Ti_2O_7$ pyrochlore powders using the sol-gel method. Rare earth nitrate salts and titanium isopropoxide sol were prepared separately in DI water and mixed. Citric acid was separately mixed with ethanol and stirred for 30 min before adding to the above mixture with continuous stirring to obtain a transparent solution. The mixture solution was dried at 60°C and calcinated at 800°C for 3 h.

The comparison of all the synthesis processes based on various parameters are presented in Table 4.

Table 4. Synthesis process comparison

Parameters	Synthesis method				
	Solid state reaction	**Coprecipitation**	**Hydrothermal**	**Sol-gel**	**Combustion**
Approach	Top-down	Bottom-up	Bottom-up	Bottom-up	Bottom-up
Reaction parameters	Temperature, Time	pH, Temperature	Pressure, Temperature, pH	Surfactant, pH, Temperature	Fuel, Stabilizer, Temperature
Precursors	Rare earth oxides	Rare earth chloride and nitrate salts	Rare earth chloride and nitrite salts, rare earth oxides	Rare earth chloride and nitrate salts, rare earth isopropoxide	Rare earth nitrates
Particle size and shape	No uniform shape and size	Uniform shape not in uniform size	Uniform shape and size	No uniform shape and size	No uniform shape and size
Porosity	Low porosity	Low porosity	No porosity	Porous	Highly porous
Reaction duration	High	Moderate	Low	Moderate	Moderate
Calcination/ Heat treatment	Required	Required	Not required	Required	Required
Process reaction rate acceleration	Not possible	pH increase	Microwave assisted hydrothermal synthesis, pH	pH, surfactant	pH, stabilizer

3. Conclusions

The various synthesis techniques available to prepare the rare earth-based pyrochlore-structured materials have been discussed. Most of the commercial applications found use a solid-state reaction synthesis method, which is suitable for producing the larger quantity of the pyrochlores. The solid-

state reaction method produces pyrochlore-based material of a single phase. Drawbacks of this method are that this method consumes enormous time, produces no dimensional homogeneity and consumes a lot of energy. Wet chemical synthesis is an alternate method to solid-state synthesis, where the synthesis is possible at a lower temperature, and the synthesized powders have homogeneous particle distribution, unique crystalline structure with excellent physical as well as mechanical properties. Hydrothermal synthesis is one of the wet chemical methods in which the use of water at supercritical pressure can synthesize rare earth-based pyrochlores at less than 400°C with a uniform crystalline structure, and particle distribution with uniform morphology. The featured work was aimed for the mass production of rare earth-based pyrochlore-structured materials via hydrothermal synthesis possibilities for high efficiency and good yield.

References

[1] Zhang, J., Guo, X., Jung, Y.G., Li, L. and Knapp, J., 2017. Lanthanum zirconate based thermal barrier coatings: A review. *Surface and Coatings Technology*, 323, 18-29.

[2] Liu, B., Liu, Y., Zhu, C., Xiang, H., Chen, H., Sun, L., Gao, Y. and Zhou, Y., 2019. Advances on strategies for searching for next generation thermal barrier coating materials. *Journal of Materials Science and Technology*, 35(5), 833-851.

[3] Schmitt, M.P., Stokes, J.L., Rai, A.K., Schwartz, A.J. and Wolfe, D.E., 2019. Durable aluminate toughened zirconate composite thermal barrier coating (TBC) materials for high temperature operation. *Journal of the American Ceramic Society*, 102(8), 4781-4793.

[4] Cernuschi, F., Bianchi, P., Leoni, M. and Scardi, P., 1999. Thermal diffusivity/microstructure relationship in Y-PSZ thermal barrier coatings. *Journal of Thermal Spray Technology*, 8(1), 102-109.

[5] Cao, X.Q., Vassen, R. and Stöver, D., 2004. Ceramic materials for thermal barrier coatings. *Journal of the European Ceramic Society*, 24(1), 1-10.

[6] Garvie, R.C., 1970. Zirconium dioxide and some of its binary systems. *Refractory Materials*, 5, 117-166.

[7] Vassen, R., Cao, X., Tietz, F., Kerkhoff, G. and Stoever, D., 1999. $La_2Zr_2O_7$-a new candidate for thermal barrier coatings. *Proceedings of the United Thermal Spray Conference-UTSC'99*, DVS-Verlag, Düsseldorf, Germany, 1999, 830-834.

[8] Samsonov, G.V., 1982. *The Oxide Handbook*. New York: Springer.

[9] Ramaswamy, P., Seetharamu, S., Rao, K.J. and Varma, K.B.R., 1998. Thermal shock characteristics of plasma sprayed mullite coatings. *Journal of Thermal Spray Technology*, 7(4), 497-504.

[10] Xu, H., Guo, H., Liu, F. and Gong, S., 2000. Development of gradient thermal barrier coatings and their hot-fatigue behavior. *Surface and Coatings Technology*, 130(1), 133-139.

[11] Warshaw, I. and Roy, R., 1961. Polymorphism of the rare earth sesquioxides1. *The Journal of Physical Chemistry*, 65(11), 2048-2051.

[12] Chuanxian, D. and Zhaohe, T., 1992. Laboratory report-thermal spraying at the Shanghai Institute of Ceramics. *Journal of Thermal Spray Technology*, 1(3), 205-209.

[13] Chen, X., Zhao, Y., Fan, X., Liu, Y., Zou, B., Wang, Y., Ma, H. and Cao, X., 2011. Thermal cycling failure of new $LaMgAl_{11}O_{19}$/YSZ double ceramic top coat thermal barrier coating systems. *Surface and Coatings Technology*, 205(10), 3293-3300.

[14] Karthik, A., Srither, S.R., Dhineshbabu, N.R., Lenin, N., Arunmetha, S., Manivasakan, P. and Rajendran, V., 2019. Stabilization of tetragonal zirconia in alumina-zirconia and alumina-yttria stabilized zirconia nanocomposites: A comparative structural analysis. *Materials Characterization*, 158, https://doi.org/10.1016/j.matchar.2019.109964.

[15] Zhou, X., Song, W., Yuan, J., Gong, Q., Zhang, H., Cao, X. and Dingwell, D.B., 2020. Thermophysical properties and cyclic lifetime of plasma sprayed $SrAl_{12}O_{19}$ for thermal barrier coating applications. *Journal of the American Ceramic Society*, 103, 5599-5611.

[16] Northam, M., 2019. *Investigation of PS-PVD and EB-PVD thermal barrier coatings over lifetime using synchrotron X-ray diffraction.*MS. University of Central Florida.

[17] Gan, X., Yu, Z., Yuan, K., Xu, C., Zhang, G., Wang, X., Zhu, L. and Xu, D., 2018. Effects of cerium addition on the microstructure, mechanical properties and thermal conductivity of YSZ fibers. *Ceramics International*, 44(6), 7077-7083.

[18] Venkadesan, G. and Muthusamy, J., 2019. Experimental investigation of Al_2O_3/8YSZ and CeO_2/8YSZ plasma sprayed thermal barrier coating on diesel engine. *Ceramics International*, 45(3), 3166-3176.

[19] Keyvani, A., Bahamirian, M. and Kobayashi, A., 2017. Effect of sintering rate on the porous microstructural, mechanical and thermomechanical properties of YSZ and CSZ TBC coatings undergoing thermal cycling. *Journal of Alloys and Compounds*, 727, 1057-1066.

[20] Anantharaman, A.P. and Dasari, H.P., 2020. Potential of pyrochlore structure materials in solid oxide fuel cell applications. *Ceramics International*, https://doi.org/10.1016/j.ceramint.2020.10.012.

[21] Cao, X.Q., Vassen, R., Jungen, W., Schwartz, S., Tietz, F. and Stöver, D., 2001. Thermal stability of lanthanum zirconate plasma-sprayed coating. *Journal of the American Ceramic Society*, 84(9), 2086-2090.

[22] Lei, M.A., Weimin, M.A., Xudong, S.U.N., Jianan, L.I.U., Lianyong, J.I. and Han, S.O.N.G., 2015. Structure properties and sintering densification of $Gd_2Zr_2O_7$ nanoparticles prepared via different acid combustion methods. *Journal of Rare Earths*, 33(2), 195-201.

[23] Mandal, B.P., Shukla, R., Achary, S.N. and Tyagi, A.K., 2010. Crucial role of the reaction conditions in isolating several metastable phases in a Gd− Ce− Zr− O system. *Inorganic Chemistry*, 49(22), 10415-10421.

[24] Vaßen, R., Jarligo, M.O., Steinke, T., Mack, D.E. and Stöver, D., 2010. Overview on advanced thermal barrier coatings. *Surface and Coatings Technology*, 205(4), 938-942.

[25] Ma, W., Meng, X., Dong, H., Lun, W. and Zheng, X., 2013. Double rare-earth oxides co-doped strontium zirconate as a new thermal barrier coating material. *Journal of Thermal Spray Technology*, 22, 104-109

[26] Ma, W., Meng, X., Wen, J., Li, E., Bai, Y., Chan, W. and Dong, H., 2019. Aging effect on microstructure and property of strontium zirconate coating co-doped with double rare-earth oxides. *Journal of the American Ceramic Society*, 102, 2143-2153.

[27] Zhong, X., Zhao, H., Liu, C., Wang, L., Shao, F., Zhou, X., Tao, S. and Ding, C., 2015. Improvement in thermal shock resistance of gadolinium zirconate coating by addition of nanostructured yttria partially-stabilized zirconia. *Ceramics International*, 41(6), 7318-7324.

[28] Zhou, D., Mack, D.E., Bakan, E., Mauer, G., Sebold, D., Guillon, O. and Vaßen, R., 2020. Thermal cycling performances of multilayered yttria-stabilized zirconia/gadolinium zirconate thermal barrier coatings. *Journal of the American Ceramic Society*, 103(3), 2048-2061.

[29] Lehmann, H., Pitzer, D., Pracht, G., Vassen, R. and Stöver, D., 2003. Thermal conductivity and thermal expansion coefficients of the lanthanum rare-earth-element zirconate system. *Journal of the American Ceramic Society*, 86(8), 1338-1344.

[30] Zhong, X., Zhao, H., Zhou, X., Liu, C., Wang, L., Shao, F., Yang, K., Tao, S. and Ding, C., 2014. Thermal shock behavior of toughened gadolinium zirconate/YSZ double-ceramic-ayered thermal barrier coating. *Journal of Alloys and Compounds*, 593, 50-55.

[31] Ma, W., Lun, W., Dong, H., Wang, L., Song, F. and Zheng, X., 2011. Fundamental physical properties of Ta_2O_5 and Yb_2O_3 codoped strontium zirconate for thermal barrier coating applications. *Materials Research Innovations*, 15(5), 319-323.

[32] Li, J.Y., Dai, H., Zhong, X.H., Zhang, Y.F., Ma, X.F., Meng, J. and Cao, X.Q., 2008. Lanthanum zirconate ceramic toughened by $BaTiO_3$ secondary phase. *Journal of Alloys and Compounds*, 452(2), 406-409.

[33] Hu, Q., Zeng, J., Wang, L., Shu, X., Shao, D., Zhang, H. and Lu, X., 2018. Helium ion irradiation effects on neodymium and cerium co-doped $Gd_2Zr_2O_7$ pyrochlore ceramic. *Journal of Rare Earths*, 36(4), 398-403.

[34] Mazilin, I.V., Baldaev, L.K., Drobot, D.V., Marchukov, E.Y. and Akhmetgareeva, A.M., 2016. Composition and structure of coatings based on rare-earth zirconates. *Inorganic Materials*, 52(9), 939-944.

[35] Pasupuleti, K.T., Prasad, G.V., Akhil, M.P., Ramaswamy, P. and Murty, S.N., 2019. Adhesion strength studies on zirconia based pyrochlore and functionally gradient thermal barrier coatings. *Materials Today: Proceedings*, 19, 568-574.

[36] Wang, Y., Zhang, L., Wu, W. and Yang, J., 2019. Enhancement of thermal properties of ytterbium-cerium oxide by zirconium doping for thermal barrier coatings. *Philosophical Magazine Letters*, 99(9), 309-316.

[37] Ma, W., Meng, X., Wen, J., Li, E., Bai, Y., Chen, W. and Dong, H., 2019. Aging effect on microstructure and property of strontium zirconate coating co-doped with double rare-earth oxides. *Journal of the American Ceramic Society*, 102(4), 2143-2153.

[38] Yang, J., Zhao, M., Zhang, L., Wang, Z. and Pan, W., 2018. Pronounced enhancement of thermal expansion coefficients of rare-earth zirconate by cerium doping. *Scripta Materialia*, 153, 1-5.

[39] Pasupuleti, K.T., Ghosh, S., Dunna, U.M., Ramaswamy, P. and Murty, S.N., 2019. Influence of atmospheric plasma spray process parameters on crystal and micro structures of pyrochlore phase in rare earth zirconate thermal barrier coatings. *Materials Today: Proceedings*, 19, 731-736.

[40] Zhang, C., Zhao, J., Yang, L., Zhou, Y., Wang, Q., Chen, H., Yang, G., Gao, Y. and Liu, B., 2020. Preparation and corrosion resistance of nonstoichiometric lanthanum zirconate coatings. *Journal of the European Ceramic Society*, 40(8), 3122-3128.

[41] Liu, Z.G., Ouyang, J.H., Zhou, Y., Li, J. and Xia, X.L., 2009. Influence of ytterbium-and samarium-oxides codoping on structure and thermal conductivity of zirconate ceramics. *Journal of the European Ceramic Society*, 29(4), 647-652.

[42] Zhou, D., Mack, D.E., Bakan, E., Mauer, G., Sebold, D., Guillon, O. and Vaßen, R., 2020. Thermal cycling performances of multilayered yttria-stabilized zirconia/gadolinium zirconate thermal barrier coatings. *Journal of the American Ceramic Society*, 103, 2048-2061.

[43] Gentleman, M.M., and Clarke, D.R., 2005. Luminescence sensing of temperature in pyrochlore zirconate materials for thermal barrier coatings. *Surface and Coatings Technology*, 200(5-6), 1264-1269.

[44] Torres-Rodriguez, J., Gutierrez-Cano, V., Menelaou, M., Kaštyl, J., Cihlář, J., Tkachenko, S., González, J.A., Kalmár, J., Fábián, I., Lázár, I. and Čelko, L., 2019. Rare-earth zirconate $Ln_2Zr_2O_7$ (Ln: La, Nd, Gd, and Dy) powders, xerogels, and aerogels: preparation, structure, and properties. *Inorganic Chemistry*, 58(21), 14467-14477.

[45] Benčina, M. and Valant, M., 2018. $Bi_2Ti_2O_7$-based pyrochlore nanoparticles and their superior photocatalytic activity under visible light. *Journal of the American Ceramic Society*, 101(1), 82-90.

[46] Gupta, S.K., Zuniga, J.P., Ghosh, P.S., Abdou, M. and Mao, Y., 2018. Correlating structure and luminescence properties of undoped and Eu^{3+}-doped $La_2Hf_2O_7$ nanoparticles prepared with different coprecipitating pH values through experimental and theoretical studies. *Inorganic Chemistry*, 57, 11815-11830.

[47] Kaliyaperumal, C., Sankarakumar, A., Palanisamy, J. and Paramasivam, T., 2018. Fluorite to pyrochlore phase transformation in nanocrystalline $Nd_2Zr_2O_7$. *Materials Letters*, 228, 493-496.

[48] Pokhrel, M., Gupta, S.K., Wahid, K. and Mao, Y., 2019. Pyrochlore rare-earth hafnate $RE_2Hf_2O_7$ (RE= La and Pr) nanoparticles stabilized by molten-salt synthesis at low temperature. *Inorganic Chemistry*, 58(2), 1241-1251.

[49] Popov, V.V., Menushenkov, A.P., Ivanov, A.A., Yastrebtsev, A.A., Gaynanov, B.R., Acapito, F. and Puri, A., 2020. A XAFS investigation of amorphous-to-crystalline and fluorite-to-pyrochlore phase transitions in $Ln_2M_2O_7$ (Ln = Gd, Tb, Dy; M = Ti, Zr). *Radiation Physics and Chemistry*, 175, 108469.

[50] Wang, Z., Zhu, H., Ai, L., Liu, X., Lv, M., Wang, L., Ma, Z. and Zhang, Z., 2016. Catalytic combustion of soot particulates over rare-earth substituted $Ln_2Sn_2O_7$ pyrochlores (Ln= La, Nd and Sm). *Journal of Colloid and Interface Science*, 478, 209-216.

[51] Matovic, B., Maletaskic, J., Zagorac, J., Pavkov, V., Maki, R.S., Yoshida, K. and Yano, T., 2020. Synthesis and characterization of pyrochlore lanthanide (Pr, Sm) zirconate ceramics. *Journal of the European Ceramic Society*, 40(7), 2652-2657.

[52] Venkatesh, G., Subramanian, R. and Berchmans, L.J., 2019. Phase analysis and microstructural investigations of $Ce_2Zr_2O_7$ for high-temperature coatings on Ni-base superalloy substrates. *High Temperature Materials and Processes*, 38(2019), 773-782.

[53] Li, W., Zhang, K., Xie, D., Deng, T., Luo, B., Zhang, H. and Huang, X., 2020. Characterizations of vacuum sintered $Gd_2Zr_2O_7$ transparent ceramics using combustion synthesized nanopowder. *Journal of the European Ceramic Society*, 40(4), 1665-1670.

[54] Jeyasingh, T., Saji, S.K. and Wariar, P.R.S., 2017. Synthesis of nanocrystalline $Gd_2Ti_2O_7$ by combustion process and its structural, optical and dielectric properties. *AIP Conference Proceedings*, 1859(1), https://doi.org/10.1063/1.4990169

[55] Jeyasingh, T., Saji, S.K., Kavitha, V.T. and Wariar, P.R.S., 2018. Frequency dependent dielectric properties of combustion synthesized $Dy_2Ti_2O_7$ pyrochlore oxide. *AIP Conference Proceedings*, 1953(1), https://doi.org/10.1063/1.5032442

[56] Ai, L., Wang, Z., Cui, C., Liu, W. and Wang, L., 2018. Catalytic oxidation of soot on a novel active Ca-Co dually-doped lanthanum tin pyrochlore oxide. *Materials*, 11(5), 653, https://doi.org/10.3390/ma11050653.

[57] Jeyasingh, T., Vindhya, P.S., Saji, S.K., Wariar, P.R.S. and Kavitha, V.T., 2019. Structural and magnetic properties of combustion synthesized $A_2Ti_2O_7$(A = Gd, Dy and Y) pyrochlore oxides. *Bulletin of Materials Science*, 42(5), https://doi.org./10.1007/s12034-019-1878-1.

[58] Quader, A., Mustafa, G.M., Abbas, S.K., Ahmad, H., Riaz, S., Naseem, S. and Atiq, S., 2020. Efficient energy storage and fast switching capabilities in Nd-substituted $La_2Sn_2O_7$ pyrochlores. *Chemical Engineering Journal*, 396, https://doi.org/10.1016/j.cej.2020.125198

[59] Zhang, K.Q., Liu, C.G., Li, F.Z., Yang, D.Y., Chen, C., Wu, R.D., Peng, S.M., Li, Y.H. and Zhang, H.B., 2016. Study on the crystal structure of $(Gd_{2-x}Ce_x)Ti_2O_7$ ($0 \leq x \leq 0.8$) pyrochlore. *Advances in Applied Ceramics*, 115(7), 411-416.

[60] Wang, Q., Cheng, X., Li, J. and Jin, H., 2016. Hydrothermal synthesis and photocatalytic properties of pyrochlore $Sm_2Zr_2O_7$ nanoparticles. *Journal of Photochemistry and Photobiology A: Chemistry*, 321, 48-54.

[61] Hongming, Z. and Danqing, Y., 2008. Effect of rare earth doping on thermo-physical properties of lanthanum zirconate ceramic for thermal barrier coatings. *Journal of Rare Earths*, 26, 770-774.

[62] Huo, Y., Qin, N., Liao, C., Feng, H., Gu, Y. and Cheng, H., 2019. Hydrothermal synthesis and energy storage performance of ultrafine $Ce_2Sn_2O_7$ nanocubes. *Journal of Central South University*, 26(6), 1416-1425.

[63] Gadipelly, T., Dasgupta, A., Ghosh, C., Krupa, V., Sornadurai, D., Sahu, B.K. and Dhara, S., 2020. Synthesis and structural characterisation of $Y_2Ti_2O_7$ using microwave hydrothermal route. *Journal of Alloys and Compounds*, 814, https://doi.org/10.1016/j.jallcom.2019.152273.

[64] Sanjeewa, L.D., Ross, K.A., Sarkis, C.L., Nair, H.S., McMillen, C.D. and Kolis, J.W., 2018. Single crystals of cubic rare-earth pyrochlore germanates: $RE_2Ge_2O_7$ (RE= Yb and Lu) grown by a high-temperature hydrothermal technique. *Inorganic Chemistry*, 57(20), 12456-12460.

[65] Trujillano, R., Martín, J.A. and Rives, V., 2016. Hydrothermal synthesis of $Sm_2Sn_2O_7$ pyrochlore accelerated by microwave irradiation. A comparison with the solid state synthesis method. *Ceramics International*, 42(14), 15950-15954.

[66] Verma, S., Rani, S. and Kumar, S., 2018. Crystal structure, morphology and optical behaviour of sol-gel derived pyrochlore rare earth titanates $RE_2Ti_2O_7$ (RE=Dy, Sm). *Journal of Alloys and Compounds*, 750, 902-910.

[67] Wang, S., Li, W., Wang, S., Zhang, J. and Chen, Z., 2016. Deposition of SiC/$La_2Zr_2O_7$ multi-component coating on C/SiC substrate by combining sol-gel process and slurry. *Surface and Coatings Technology*, 302, 383-388.

[68] Xia, J., Lei, L., Dai, X., Ling, J., Li, Y. and Xu, S., 2018. Excitation-dependent multi-color emissions in Yb/Er/Eu: $Gd_2Ti_2O_7$ pyrochlore for anti-counterfeiting. *Materials Research Bulletin*, 107, 213-217.